International Journal of Advances in Applied Sciences (IJAAS)
Vol. 15, No. 1, March 2026, pp. 281~292
ISSN: 2252-8814, DOI: 10.11591/ijaas.v15.i1.pp281-292

DCNNVA: a deep convolutional neural network for volcanic activity classification using satellite imagery

Yasir Hussein Shakir[1], Reem Ali Mutlag[1], Eshaq Aziz Awadh AL Mandhari[2], Mohamed Shabbir Abdulnabi[3]
[1]College of Graduate Studies, Universiti Tenaga Nasional, Kajang, Malaysia
[2]Graduate School of Technology, Asia Pacific University of Technology and Innovation, Kuala Lumpur, Malaysia
[3]School of Technology, Asia Pacific University of Technology and Innovation, Kuala Lumpur, Malaysia

Article Info

Article history:

Received Sep 4, 2025
Revised Dec 23, 2025
Accepted Jan 1, 2026

Keywords:

DCNNVA
Deep learning
Model deployment
Multi-modal alert system
Satellite data classification

ABSTRACT

Monitoring and classifying volcanic activity are a critical task for disaster risk reduction and hazard management. Recent discoveries in machine learning and deep learning have proved excellent satellite image classification and volcanic anomaly identification capabilities, yet the majority of existing methods suffer from small datasets, particularly on solitary data modalities or particular cases, merely as examples. In this research work, we put forward develop deep convolutional neural network for volcanic activity (DCNNVA) classification specifically designed for satellite imagery on volcanic activity. We rigorously benchmarked DCNNVA model's strength against a total of eight state-of-the-art transfer learning models: ResNet50, NASNetLarge, DenseNet121, MobileNet, InceptionV3, Xception, VGG19, and VGG16. Comparative experimental results show that proposed DCNNVA framework's overall performance significantly surpasses its competitors with an accuracy of 99.33%, precision of 100%, recall of 98.67%, and F1-score of 99.33%, significantly beating existing state-of-the-art methods. Also, we create a deployable graphical user interface (GUI) system that is capable of real-time monitoring on volcanic activity and generates multi-modal alert processing that can make this research directly applicable for practical use on disaster management as well as in early warning systems. This research contributes a scalable, strong, as well as practical solution towards volcanic hazard identification as well as a baseline system toward developing future multi-modal as well as real-time geohazard tracking system frameworks.

Corresponding Author:

Mohamed Shabbir Abdulnabi
School of Technology, Asia Pacific University of Technology and Innovation
Kuala Lumpur 57000, Malaysia
Email: mohamed.shabbir@apu.edu.my

1. INTRODUCTION

Monitoring and classifying volcanic events are widely recognized as one of the most critical yet challenging responsibilities faced via observatories and geoscientific institutions around the world. The volcanic activity presents not only a significant natural hazard to human populations and infrastructure but also a fundamental area of study for understanding earth dynamic systems. Traditionally, the observation and analysis of volcanic activity have relied heavily on ground-based monitoring systems, manual image interpretation, and conventional statistical models. However, these approaches were often limited by temporal delays restricted coverage, and the high costs associated with on-site monitoring. The rapid

advancement of remote sensing technologies, especially the growing availability of high-resolution multispectral and thermal satellite imagery, has greatly expanded the ability of researchers to monitor volcanic activity at both local and global scales. Supported by increased computational power, these tools now allow large-scale data processing and real-time monitoring capabilities that were previously unattainable using traditional approaches [1]. At the same time, artificial intelligence has emerged as a transformative approach for handling complex high-dimensional datasets, and with machine learning and deep learning techniques have shown exceptional effectiveness in solving problems related to image classification, anomaly detection, and predictive modeling [2], [3].

A major research focus was the classification of satellite imagery, which plays a crucial role in detecting subtle thermal anomalies, gas emissions, land cover shifts, and other indicators of volcanic activity. Recent work has shown that immune-inspired machine learning algorithms and other models can significantly boost classification accuracy even when datasets are noisy or limited [4]. Among deep learning models, convolutional neural networks (CNNs) stand out as one of the most effective techniques for remote sensing applications. CNNs have a unique capability to automatically extract hierarchical and spatial features from images, which allows them to surpass traditional methods that rely on handcrafted features [5]. This strength is especially important in volcanic monitoring, where detecting subtle spatiotemporal patterns can be critical for identifying early signs of activity. In addition, the use of transfer learning has further improved CNN performance. Models that have been pre-trained on large-scale datasets such as ImageNet can be fine-tuned for volcanic image classification. This approach significantly reduces the requirement for large amounts of domain-specific training data while simultaneously boosting classification accuracy [6], [7]. Such approaches are particularly valuable in volcanic monitoring, where annotated datasets are scarce and imbalanced. Despite significant progress, existing methods face challenges related to scalability, generalization across different volcanoes, and the integration of multimodal satellite data. Artificial intelligence methods and pixel-based classifiers have shown potential, but their application to volcanic activity remains limited.

The contributions are thus concluded to be as follows:

i) Introduces a deep learning-based framework for volcanic activity classification using a custom-designed develop deep convolutional neural network for volcanic activity (DCNNVA) architecture.
ii) Comprehensive model evaluation via eight state-of-the-art transfer learning models, such as ResNet50, NASNetLarge, DenseNet121, MobileNet, InceptionV3, Xception, VGG19, and VGG16.
iii) Enhanced model robustness via data augmentation techniques and extensive experimental validation uses multiple performance metrics.
iv) Deployable graphical user interface (GUI) system that provides real-time volcanic activity monitoring with multi-modal alert capabilities, making the research practically applicable for disaster management.

The structure of this paper is outlined as follows: section 2 presents the related work, reviewing previous studies and recent developments relevant to this research area. Section 3 the materials and methods, provides details of the architecture, methodology, datasets, pre-processing, dividing data, investigated models, and evaluation metrics. Section 4 results and discussion with comparisons to related studies in the literature. Finally, section 5 presents the conclusions.

2. RELATED WORK

Recent research has explored the use of machine learning and deep learning for satellite image classification and volcanic activity monitoring. Early studies applied pixel-based machine learning; similarly, Ebrahimy and Zhang [8] increased classification accuracy by applying various extreme learning machine classifiers together. Ouchra *et al.* [9] compared supervised and unsupervised machine learning techniques of urban land covering classification by employing Landsat 8 imagery and emphasized methodological differences applied to feature extraction. In volcanic contexts, Cariello *et al.* [10] showed the application of machine learning to Sentinel-2 imagery to track volcanic thermal anomalies, while Buttar and Sachan [11] utilized ResNet-152 to classify and geo-image images with a focus on the requirement of automated feature extraction. Corradino *et al.* [12] utilized U-NET to analyze 21 years of advanced spaceborne thermal emission and reflection radiometer (ASTER) global thermal infrared (TIR) imagery of five volcanoes and attained 93% effectiveness of anomaly detection. Similarly, Shultz [13] presented the CNN-based frame, hotspot learning and identification network (HotLINK), tested and proved with moderate resolution imaging spectroradiometer (MODIS) and visible infrared imaging radiometer suite (VIIRS) data collections, and attained over 95% accuracy of hotspot identification.

Other approaches have used CNNs in non-image domains. Oñate *et al.* [14] forecasted micro-earthquakes using manifold learning and audio-driven features, and achieved over 94% accuracy. Nunnari and Calvari [15] contrasted eight CNN models for eruptive activity monitoring of Mount Etna and

established transfer learning as superior. Chen *et al.* [16] proposed transfer learning-based VGG (TVGG) for remote sensing image classification with 99.18% accuracy based on a VGG-based transfer learning technique. Mohan *et al.* [17] introduced Hotspotter, an end-to-end system designed to automatically detect subtle volcanic thermal anomalies in satellite imagery while also generating key thermal statistics. Earlier methods for automated volcanic thermal feature (VTF) detection were limited by small datasets and narrow geographic coverage. The Reed-Xiaoli algorithm (LRX)+CNN approach, which trained CNN for 50 epochs on the LRX score images, produced an F1-score of 88.4% and a test accuracy of 90.3%. Huertas *et al.* [18] developed VGG16 and Inception CNN models to analyze mud volcano imagery and findings show that both transfer learning and custom CNNs are well-suited for handling the challenges of this type of data. The VGG16 model achieved test accuracy of 93%, with precision and recall scores of 93% and 94% for the "mud" class and 93% and 93% for the "no mud" class. The Inception model also demonstrated stable performance with only minor variation.

In summary, the studies to date have utilized several various datasets and variety of machine learning and deep learning algorithms techniques to volcanic monitoring and satellite image classification. While these approaches demonstrate significant progress, most remain at the experimental stage and lack practical deployment. In particular no existing research has proposed a comprehensive framework that integrates a deployable GUI with real-time volcanic activity monitoring and multi-modal alerting capabilities features that are essential for effective disaster management applications. Furthermore, many studies are constrained by limited datasets and inconsistent performance across different contexts, highlighting the need for more robust, scalable, and practically applicable solutions. A comparative analysis of the previous related work is presented in tabular form in Table 1.

Table 1. Summary of recent machine learning and deep learning for volcanic satellite image classification

Reference/year	Dataset	Methods	Results (%)	Weakness
Corradino *et al.* [12], 2024	21 years of ASTER TIR data (5 volcanoes)	CNN (U-NET architecture)	Accuracy =93	Limited to ASTER TIR imagery, model generalizability to other sensors not tested.
Shultz [13], 2024	VIIRS and MODIS imagery (Alaskan volcanoes)	CNN (HotLINK)	Accuracy =98	Dataset geographically restricted (Alaska), limited validation on diverse volcanic settings.
Oñate *et al*. [14], 2024	Seismic data (Cotopaxi and Llaima)	Audio features+psychoacoustic scales+manifold learning	Accuracy =94.44–95.45	Focused on seismic data only, lacks multi-modal integration with satellite imagery.
Nunnari and Calvari [15], 2024	Ground-based thermal images (Mt. Etna)	Comparison of 8 CNNs (SqueezeNet, GoogleNet, DenseNet201, ResNet18, ShuffleNet, DarkNet19, AlexNet, VGG-16)	Accuracy =94.07	Results restricted to one volcano, computationally expensive due to multiple CNN comparisons.
Chen *et al*. [16], 2024	Tiangong-2 remote sensing dataset	TVGG (from ImageNet)	Accuracy =99.18 Recall =99.17	Relies heavily on transfer learning and lacks testing on volcanic datasets.
Mohan *et al*. [17], 2025	Thermal satellite data	LRX+CNN (50 epochs)	Accuracy =90.30 F1-score =88.40	Dataset relatively small, performance lower than other CNN-based models.
Huertas *et al.* [18], 2025	INGV (mud volcano imagery)	VGG16 and Inception CNN	Accuracy =93 Precision =93 Recall =94	Focus limited to mud volcanoes; performance stability across broader datasets not assessed.

3. MATERIALS AND METHODS

This section contains the materials and methods framework used in this study, which is visually summarized in Figure 1. The methodology is structured into six main steps: data acquisition, data preprocessing, data division, model development and training, evaluation, and deployment.

3.1. Data acquisition

This kind of dataset consists of the images of the volcanic activity, and this has been gotten from satellite images. The following figures of several images taken from several classes of volcanoes (YesActivity) and (NoActivity) are presented in Figure 2. The complete dataset used for this experiment is publicly available online [19].

3.2. Data preprocessing

To ensure that the data was standardized and optimized for deep learning, several preprocessing steps were applied to the images, and steps were aimed at making the dataset more uniform, reducing

variability, and allowing the model to generalize more to new data. Preprocessing pipelines involved rescaling and resizing transformations, normalization of the pixels, and the application of data augmentation strategies. Data augmentation was particularly important, as it effectively increased the size of the dataset and introduced variations that simulate real-world conditions (different orientations, scales, and distortions). This helps to prevent overfitting and improve robustness, as shown in Figure 3. The augmentation was performed using the Augmentor library and the specific transformations, and their probabilities are shown in Table 2.

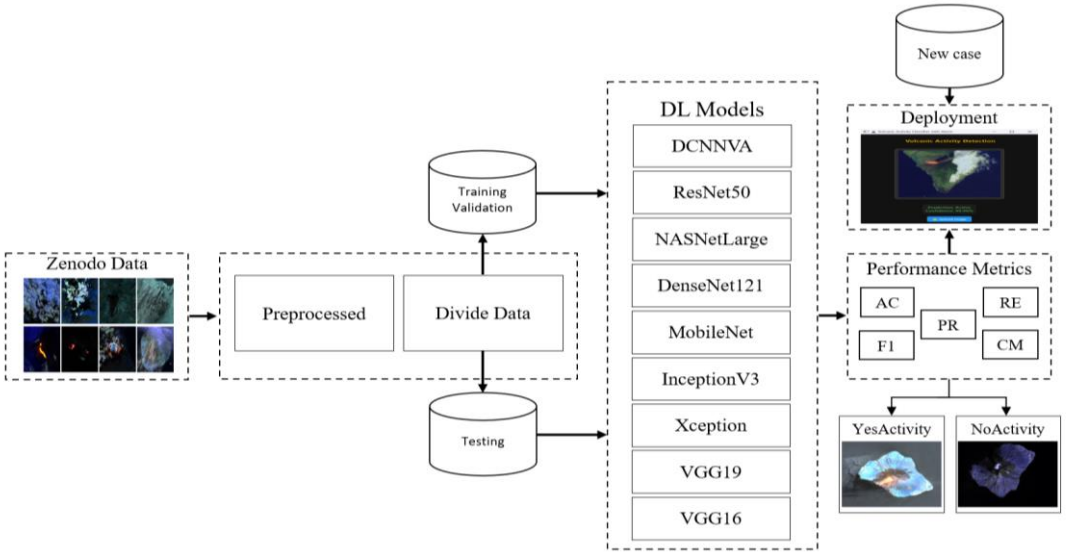

Figure 1. Proposed framework for volcanic activity classification using satellite imagery

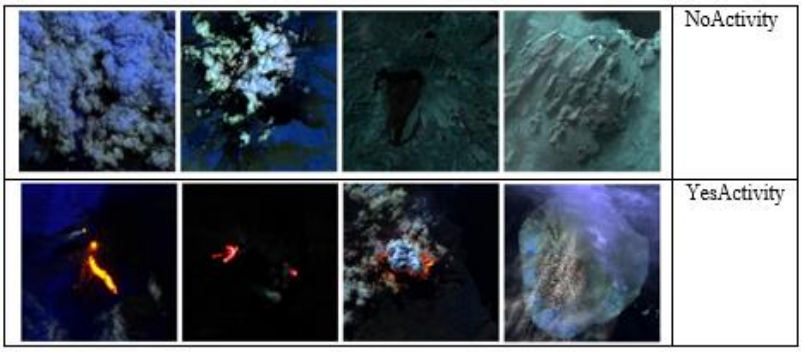

Figure 2. Sample satellite images from the 'yes activity' and 'no activity' volcanic dataset classes

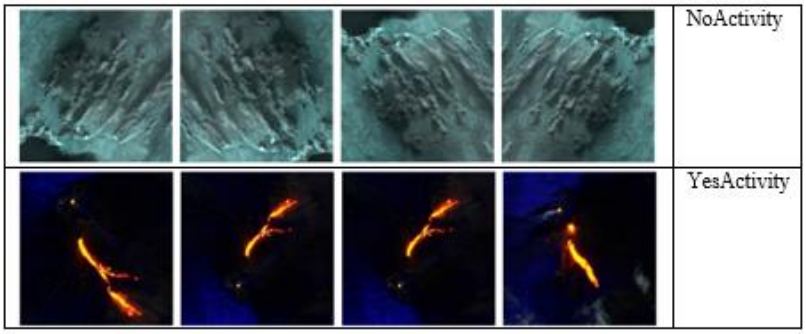

Figure 3. Illustration of data augmentation techniques applied to original volcanic images

Table 2. Data preprocessing and augmentation parameters for model training

Preprocessing step	Details
Rescaling	1/255.
Size	(224, 224).
Data augmentation	Technique.
	Flip left right: probability of 0.3.
	Flip top bottom: probability of 0.5.
	Rotate: probability of 0.5, with a maximum left and right rotation of 5 degrees.
	Zoom: probability of 0.3, with a zoom factor between 1.1 and 1.2.
	Random distortion: probability of 1, with a grid width and height of 3 and a magnitude of 5.

3.3. Data division

To prepare the dataset for training and evaluation, we divided it into training, validation, and testing subsets. The set was divided to be 75% for training (2,250 images), 15% for validation (350 images), and 20% for testing (600 images); all of these sets have two classes. The overall set had 3,000 images across two categories, as shown in Table 3.

Table 3. Dataset partitioning for model training, validation, and testing

Subset	Number of images	Percentage (%)	Number of classes
Training	2,250	75	2
Validation	350	15	2
Testing	600	20	2
Total	3,000	100	2

3.4. Deep learning models and architecture

Current breakthroughs in deep learning have immensely propelled the progress of satellite image processing, specifically regarding the identification of natural phenomena like volcanic activity. Employing CNNs and transfer learning facilitates quick feature detection from data of high dimensionality, while at the same time overcoming difficulties stemming from limited datasets with annotations. Herein, we put forward a new DCNNVA and eight pre-existing transfer learning models, ResNet50, NASNetLarge, DenseNet121, MobileNet, InceptionV3, Xception, VGG19, and VGG16, to build a complete classification system of volcanic satellite images.

3.4.1. Deep convolutional neural network for volcanic activity

Volcanic activity (DCNNVA) is a customized architecture developed only for volcanic activity classification using satellites, and the network is so designed that it maintains a balance between computation efficiency and classification accuracy, and therefore is usable for near real-time monitoring. It is a combination of space features, extracting convolution and pooling operations, and fully connected layers utilized at the time of classification (≈1.19 M trainable parameters).

i) Convolutional layers: the convolutional operation extracts hierarchical representations from input images by applying learnable kernels. Mathematically, the convolution at layer l can be expressed as presented in (1).

$$z_{i,j}^{(J)} = \sum_{m=0}^{m-1} \sum_{n=0}^{n-1} x_{i+m,j+n}^{(J-1)} \cdot w_{m,n}^{(J)} + b^{(J)} \quad (1)$$

Where $x^{(J-1)}$ represents input from the previous layer, $w^{(J)}$ is a convolutional kernel, $b^{(J)}$ is biased, and $z_{i,j}^{(J)}$ is the feature map at position (i,j). The non-linear activation function ReLU ($\sigma(z) = max(0,z)$) is applied to introduce non-linearity.

ii) Pooling layers: to reduce spatial dimensions while preserving essential features, max pooling is use pooling operation is defined in (2).

$$P_{i,j} = max_{(m,n)\in\Omega} \left(z_{i+m,j+n}\right) \quad (2)$$

Where Ω denotes the pooling region operation decreases computational complexity and controls overfitting via introducing translational invariance.

iii) Fully connected layers: the extracted features are flattened and passed to fully connected dense layers for classification. The transformation is given in (3).

$$y = \sigma(W_x + b) \quad (3)$$

Where W and b denote the weights and biases of dense layer, respectively, and σ represents the ReLU or softmax activation function, depending on layer. The final softmax classifier produces a probability over two output classes, where C =2 corresponds to the number of classes presented in (4).

$$p(y = c/x) = \frac{exp\,(z_C)}{\sum_{k=1}^{C} exp\,(z_k)}, c \in \{1,2\} \quad (4)$$

iv) Dropout and optimization: to enhance generalization, a dropout layer with rate p =0.5 was incorporated, which randomly deactivates neurons during training. The model is optimized using the Adam optimizer, which adaptively updates learning rates for each parameter. The categorical cross-entropy loss function is employed, as presented in (5).

$$\mathcal{L} = -\sum_{i=1}^{N}\sum_{c=1}^{C} y_{i,c}\ log\ \hat{y}_{i,c} \quad (5)$$

Where $y_{i,c}$ is the ground truth label and $\hat{y}_{i,c}$ is the predicted probability for class c.

The DCNNVA consists of five convolutional layers (64-256 filters), each of which is followed by max-pooling focusing on dimension reduction, a fully connected 256-neuron layer, a dropout layer, and a final output classification softmax layer. It has roughly 1.19 million trainable parameters, corresponding to a light but deep architecture friendly to scalability and efficiency. The model was optimized using the Adam optimizer with a learning rate of 0.001, and trained with the categorical cross-entropy loss function. Training was conducted with a batch size of 32 over 10 epochs, using the Google Collaboratory platform with an NVIDIA Tesla T4 GPU (16 GB). Figure 4 shows the DCNNVA architecture.

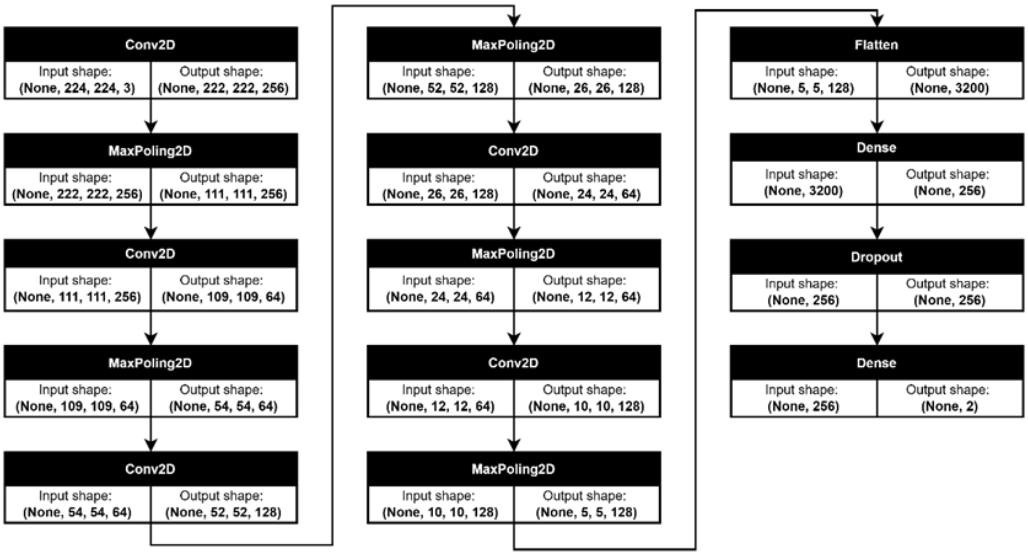

Figure 4. Architectural diagram of the proposed DCNNVA

3.4.2. ResNet50

Introduced by He *et al.* [20], ResNet50 introduces residual learning through identity shortcut connections. This mitigates the problem of vanishing gradients in deeper networks. By stacking convolutional blocks with residual links, the model enables stable training and improved feature extraction, making it well-suited for complex image classification tasks such as volcanic activity recognition.

3.4.3. NASNetLarge

NASNetLarge, introduced by Zoph *et al.* [21], is a neural architecture search (NAS)-discovered architecture that is aimed at optimizing network structures autonomously for higher performance. It is a modular architecture that utilizes reduction and normal cells. The model can achieve scalable depth and width with accuracy and computational efficiency.

3.4.4. DenseNet121

DenseNet121, introduced by Huang *et al.* [22], connects each network layer with all other network layers feed-forwardly and promotes feature reuse and efficient gradient flow. This dense connection minimizes redundancy and improves learning efficiency. It also promotes the ability of the model to identify subtle volcanic features based on satellite data.

3.4.5. MobileNet

MobileNet, presented by Howard *et al.* [23], is a lightweight CNN architecture designed specifically for mobile and embedded vision applications. By using depthwise separable convolutions and substantially decreases computation and memory requirements. It maintains accuracy, making it a likely candidate for real-time volcanic activity monitoring.

3.4.6. InceptionV3

InceptionV3, proposed by Szegedy *et al.* [24], improves the efficiency of CNNs using factorized convolutions and dimension reduction methods of the inception modules. Its architecture enables the network to achieve multi-scale feature capture at once. It also enhances volcanic image diversity-based recognition performance.

3.4.7. Xception

Xception, stated by Chollet [25], extends the Inception architecture via replacing inception modules with depthwise separable convolutions. This structure decouples spatial and channel-wise filtering. It leads to improved representational capacity and efficient training.

3.4.8. VGG19 and VGG16

VGG structured by Simonyan and Zisserman [26] (VGG16 and VGG19) are distinguished by their plainness and consistent architecture and are based on successive convolutional layers with tiny (3×3) filters. Although deep, these models are powerful in all image classification tasks. Their simple architecture also makes transfer learning feasible for detecting volcanic activity.

3.5. Evaluation performance

The trained models were assessed on the testing dataset using several performance measures, including accuracy, precision, recall, and F1-score. The formulas for all performance values are presented in (6)-(9). These values were computed using the confusion matrix shown in Table 4.

$$Accuracy = \frac{TP+TN}{TP+TN+FP+FN} \quad (6)$$

$$Precision = \frac{TP}{TP + FP} \quad (7)$$

$$Recall = \frac{TP}{TP+FN} \quad (8)$$

$$F1 - score = \frac{2 \times Precision \times Recall}{Precision + Recall} \quad (9)$$

Table 4. Structure of a confusion matrix for binary classification

	Actual positive	Actual negative
Predicted positive	True positive (TP)	False positive (FP)
Predicted negative	False negative (FN)	True negative (TN)

3.6. Deployment model

To facilitate practical utilization and demonstrate the real-world applicability of the proposed DCNNVA model, a standalone desktop application was developed. This system tool bridges the gap between experimental validation and the end-user application. It provides an intuitive platform for volcanic activity assessment.

4. RESULTS AND DISCUSSION

The experimental results clearly indicate that the new DCNNVA model greatly surpassed all transfer learning networks with a maximum accuracy 99.33% and almost perfect precision 100%, which

clearly shows that it can accurately identify volcanic activity. Its strong ability to suppress false negatives is further confirmed by its high recall value 98.67%, which is very important in early warnings regarding volcanic hazards. However, we can see that ResNet50 performed poorly with a very low accuracy level of only 68%, which we attribute to the fact that its deeper residual units are not optimal for this dataset. MobileNet, DenseNet121, and InceptionV3 performed equally well (95-96% accurate), but failed to reach the accuracy of the DCNNVA. Other older designs, such as VGG16 and VGG19, performed lower in accuracy levels compared to new architecture designs. A summary of the results is provided in Figure 5.

To better illustrate the classification performance, Figure 6 plots the confusion matrices of all algorithms. These contain a graphical representation of true positives, true negatives, false positives, and false negatives within the "volcanic activity" and "no activity" classes. Analysis of the confusion matrix confirms the superiority of the DCNNVA model, which correctly classified almost all samples but contained a negligible number of false negative 4 cases of volcanic activity misclassified as no activity. Contrary to this, numerous misclassifications were witnessed in ResNet50, primarily the absence of detection of volcanic activity in a majority of cases. MobileNet, DenseNet121, and InceptionV3 performed outstandingly but with a slightly higher misclassification rate compared to DCNNVA. The graph of training and validation accuracy of DCNNVA for ten epochs is shown in Figure 7. From the graph, the accuracy of the model increases very fast at each epoch, but slows down from epoch 4 up to the last epoch.

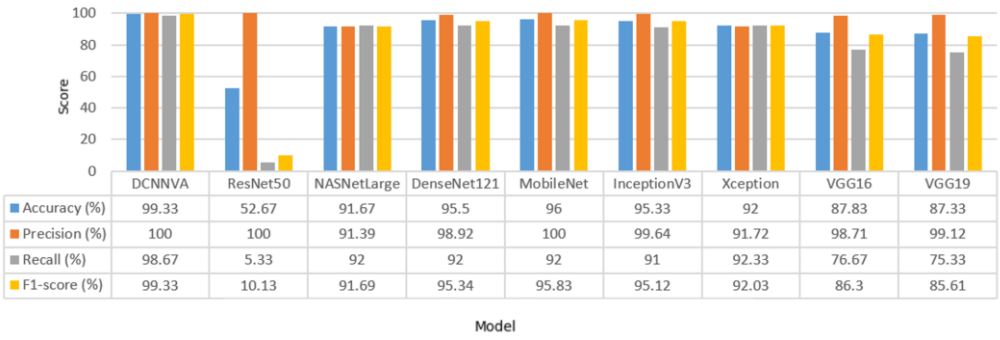

	DCNNVA	ResNet50	NASNetLarge	DenseNet121	MobileNet	InceptionV3	Xception	VGG16	VGG19
Accuracy (%)	99.33	52.67	91.67	95.5	96	95.33	92	87.83	87.33
Precision (%)	100	100	91.39	98.92	100	99.64	91.72	98.71	99.12
Recall (%)	98.67	5.33	92	92	92	91	92.33	76.67	75.33
F1-score (%)	99.33	10.13	91.69	95.34	95.83	95.12	92.03	86.3	85.61

Figure 5. Accuracy comparison of the proposed DCNNVA model against state-of-the-art

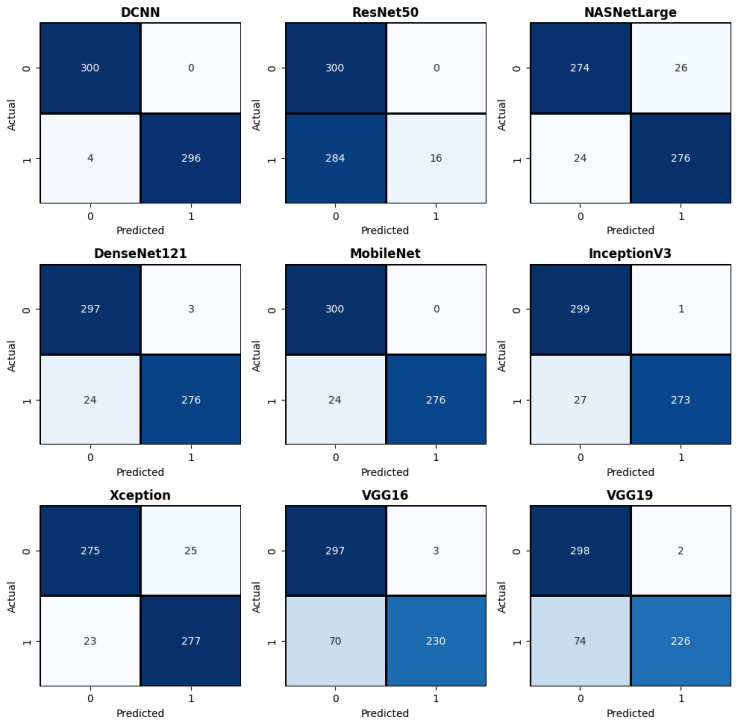

Figure 6. Confusion matrices comparing the classification performance of DCNNVA

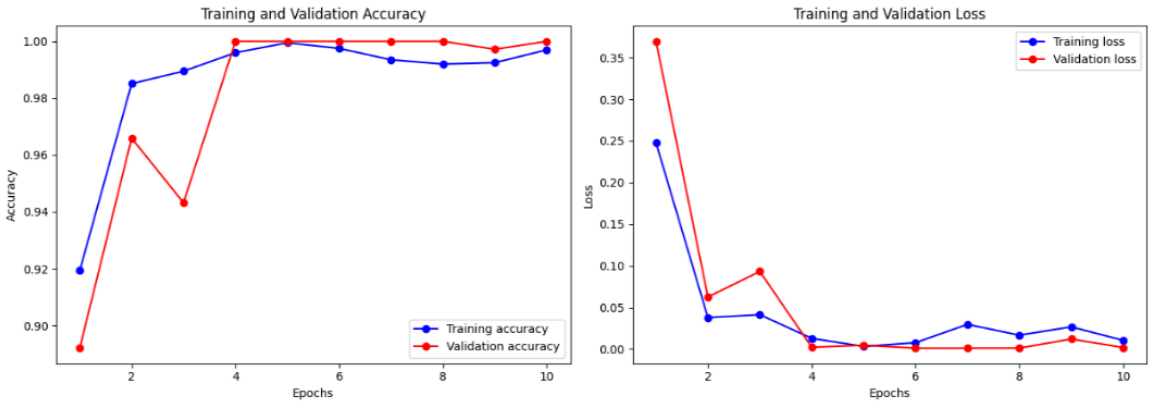

Figure 7. DCNNVA training and validation performance over 10 epochs

The superior performance of the DCNNVA model warranted its transition from a research prototype to a practical tool. To this end, a functional desktop application was developed and deployed. This application provides a user-friendly interface that allows end-users, such as geologists or monitoring station personnel, to perform real-time volcanic activity assessments. The deployment successfully demonstrates the model's operational viability. As shown in the application interface Figure 8, users can upload satellite imagery, and the system returns an instantaneous classification ("active" or "no active") accompanied by a confidence score. The interface clearly displays the prediction, for instance, "prediction: no active | confidence: 99.30%" (Figure 8(a)) or "prediction: active | confidence: 99.90%" (Figure 8(b)), providing transparent and immediate results to the operator. Crucially, the application incorporates a multi-modal alert system that, upon detecting "active" volcanic activity, triggers a clear, synthesized voice warning: "warning! volcanic activity detected." This feature is designed to capture the operator's attention immediately, which is paramount in high-stakes monitoring environments. The successful integration of the high-accuracy DCNNVA model into this deployable system underscores and also readiness for use in quasi-real-time decision-support scenarios, effectively bridging the gap between theoretical model performance and practical, on-the-ground utility.

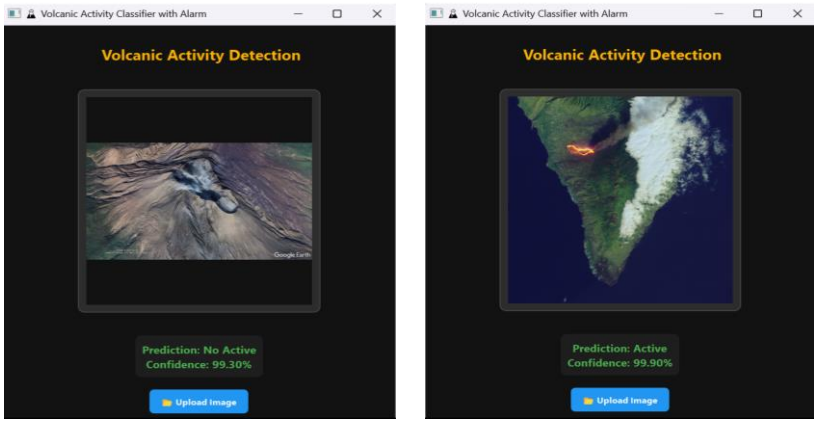

(a) (b)

Figure 8. DCNNVA application interface for volcanic activity classification of (a) "no active" (b) "active"

Furthermore, performance and practical implementation of the proposed DCNNVA model are compared to contemporary literature review in Table 5. The analysis reveals that, however various studies have achieved high accuracy, our work distinguishes two critical areas: i) achieving the best overall performance across multiple metrics and ii) successfully bridging the gap to a practical deployable tool. This practical tool features a user-friendly GUI for real-time analysis and incorporates a unique multi-modal alert system that provides immediate auditory warnings upon detection of volcanic activity. This combination of state-of-the-art predictive performance and a functional attention-grabbing deployment platform represents a significant contribution to the field of operational volcanic hazard monitoring.

Table 5. Comparative analysis of volcanic activity detection methods

Reference	Methodology	Performance (%)	Deployment	Alert system
Corradino *et al.* [12]	CNN (UNET)	Accuracy =93	Not reported	Not reported
Shultz [13]	CNN (HotLINK)	Accuracy =98	Not reported	Not reported
Oñate *et al.* [14]	Audio features + manifold learning	Accuracy =94.44 to 95.45	Not reported	Not reported
Nunnari and Calvari [15]	Comparison of 8 CNNs	Accuracy =94.07	Not reported	Not reported
Chen *et al.* [16]	TVGG	Accuracy =99.18 Recall =99.17	Not reported	Not reported
Mohan *et al.* [17]	LRX+CNN	Accuracy =90.30 F1-score =88.40	Not reported	Not reported
Huertas *et al.* [18]	VGG16 and Inception CNN	Accuracy =93 Precision =93	Not reported	Not reported
Our work	Proposed DCNNVA	Accuracy =99.33 Precision =100. Recall =98.67 F1-score =99.33	Yes (functional desktop application)	Yes (text-to-speech audio alarm)

5. CONCLUSION

In this study, a developed DCNNVA classification was rigorously validated and successfully deployed. The model was evaluated against eight state-of-the-art transfer learning architectures, including ResNet50, NASNetLarge, DenseNet121, MobileNet, InceptionV3, Xception, VGG16, and VGG19. The experimental results demonstrate that proposed DCNNVA model consistently outperformed all model networks across all evaluation metrics, achieving accuracy (99.33%), precision (100%), recall (98.67%), and F1-score (99.33%). The comprehensive analysis supported by confusion matrices and training graphs confirms the model's robust capability to minimize both false positives and false negatives, with a particularly strong performance in reducing false negatives, a critical requirement for early warning systems in volcanic hazard monitoring. Beyond theoretical performance, this research makes a substantial practical contribution through the successful development and deployment of an operational desktop application, and implementation represents a significant advancement beyond current state-of-the-art approaches, bridging the gap between experimental models and practical utility. The application features an intuitive graphical interface for real-time monitoring and incorporates a pioneering multimodal alert system that provides immediate auditory warnings upon detection of volcanic activity, a feature absents in comparable studies. Future work will aim to extend the current architecture to support multi-class classification of volcanic activity, allowing for more nuanced recognition of different eruption types, and the framework will be enhanced through the integration of multimodal data, combining information from sources such as satellites and ground-based seismic sensors. Finally, efforts will focus on deploying this system in operational monitoring networks to strengthen early warning systems and improve disaster response strategies.

FUNDING INFORMATION

Authors state no funding involved.

AUTHOR CONTRIBUTIONS STATEMENT

This journal uses the Contributor Roles Taxonomy (CRediT) to recognize individual author contributions, reduce authorship disputes, and facilitate collaboration.

Name of Author	C	M	So	Va	Fo	I	R	D	O	E	Vi	Su	P	Fu
Yasir Hussein Shakir	✓	✓	✓		✓		✓	✓		✓	✓			✓
Reem Ali Mutlag	✓		✓	✓		✓		✓	✓					
Eshaq Aziz Awadh AL Mandhari		✓		✓		✓	✓		✓		✓		✓	
Mohamed Shabbir Abdulnabi	✓	✓		✓		✓		✓		✓	✓	✓		✓

C : **C**onceptualization
M : **M**ethodology
So : **So**ftware
Va : **Va**lidation
Fo : **Fo**rmal analysis
I : **I**nvestigation
R : **R**esources
D : **D**ata Curation
O : Writing - **O**riginal Draft
E : Writing - Review & **E**diting
Vi : **Vi**sualization
Su : **Su**pervision
P : **P**roject administration
Fu : **Fu**nding acquisition

CONFLICT OF INTEREST STATEMENT

The authors declare that they have no known competing financial interests or personal relationships that could have appeared to influence the work reported in this paper.

INFORMED CONSENT

We have obtained informed consent from all individuals included in this study.

DATA AVAILABILITY

The dataset generated and analyzed during this study is openly available in the Zenodo repository at https://doi.org/10.5281/zenodo.7944343, reference number [19]. The source code and pre-trained models have been made publicly available on GitHub at https://github.com/yasserhessein/Volcanic-Activity-Monitoring-Using-Deep-Convolutional-Neural-Network-Learning-and-Satellite-Imagery.

REFERENCES

[1] K. Thangavel *et al.*, "Artificial intelligence for trusted autonomous satellite operations," *Progress in Aerospace Sciences*, vol. 144, 2024, doi: 10.1016/j.paerosci.2023.100960.

[2] M. M. Azad, S. Kim, Y. B. Cheon, and H. S. Kim, "Intelligent structural health monitoring of composite structures using machine learning, deep learning, and transfer learning: a review," *Advanced Composite Materials*, vol. 33, no. 2, pp. 162–188, 2024, doi: 10.1080/09243046.2023.2186742.

[3] M. A. Elaziz *et al.*, "Evolution toward intelligent communications: impact of deep learning applications on the future of 6G technology," *Wiley Interdisciplinary Reviews: Data Mining and Knowledge Discovery*, vol. 14, no. 1, 2024, doi: 10.1002/widm.1521.

[4] A. Rahman *et al.*, "Performance of different machine learning algorithms on satellite image classification in rural and urban setup," *Remote Sensing Applications: Society and Environment*, vol. 20, 2020, doi: 10.1016/j.rsase.2020.100410.

[5] T. T. Nguyen *et al.*, "Monitoring agriculture areas with satellite images and deep learning," *Applied Soft Computing*, vol. 95, 2020, doi: 10.1016/j.asoc.2020.106565.

[6] S. D. Khan and S. Basalamah, "Multi-branch deep learning framework for land scene classification in satellite imagery," *Remote Sensing*, vol. 15, no. 13, 2023, doi: 10.3390/rs15133408.

[7] M. Wahbi *et al.*, "A deep learning classification approach using high spatial satellite images for detection of built-up areas in rural zones: case study of Souss-Massa region-Morocco," *Remote Sensing Applications: Society and Environment*, vol. 29, 2023, doi: 10.1016/j.rsase.2022.100898.

[8] H. Ebrahimy and Z. Zhang, "Per-pixel accuracy as a weighting criterion for combining ensemble of extreme learning machine classifiers for satellite image classification," *International Journal of Applied Earth Observation and Geoinformation*, vol. 118, 2023, doi: 10.1016/j.jag.2023.103284.

[9] H. Ouchra, A. Belangour, and A. Erraissi, "Comparison of machine learning methods for satellite image classification: a case study of Casablanca using Landsat imagery and Google Earth Engine," *Journal of Environmental Earth Sciences*, vol. 3, no. 1, pp. 1–9, 2023, doi: 10.22271/27077505.2023.v3.i1a.40.

[10] S. Cariello, C. Corradino, F. Torrisi, and C. D. Negro, "Cascading machine learning to monitor volcanic thermal activity using orbital infrared data: from detection to quantitative evaluation," *Remote Sensing*, vol. 16, no. 1, 2023, doi: 10.3390/rs16010171.

[11] P. K. Buttar and M. K. Sachan, "Semantic segmentation of satellite images for crop type identification in smallholder farms," *Journal of Supercomputing*, vol. 80, no. 2, pp. 1367–1395, 2024, doi: 10.1007/s11227-023-05520-9.

[12] C. Corradino, M. S. Ramsey, S. P. -Bonnétat, A. J. L. Harris, and C. D. Negro, "Detection of subtle thermal anomalies: deep learning applied to the ASTER global volcano dataset," *IEEE Transactions on Geoscience and Remote Sensing*, vol. 61, pp. 1–15, 2023, doi: 10.1109/TGRS.2023.3241463.

[13] P. S. -Shultz, "Deep learning detection and quantification of volcanic thermal signals in infrared satellite data," *M.S. thesis*, Department of Geosciences, University of Alaska Fairbanks, Fairbanks, Alaska, 2024.

[14] C. -P. B. -Oñate, E. V. Carrera, F. -M. M. -Meseguer, R. G. -Orquera, J. L. R. -Álvarez and R. A. L. -Cueva, "Volcanic micro-earthquake classification with spectral manifolds in low-dimensional latent spaces," *IEEE Access*, vol. 12, pp. 10208–10221, 2024, doi: 10.1109/ACCESS.2024.3351234.

[15] G. Nunnari and S. Calvari, "Exploring convolutional neural networks for the thermal image classification of volcanic activity," *Geomatics*, vol. 4, no. 2, pp. 124–137, 2024, doi: 10.3390/geomatics4020007.

[16] Y. Chen, S. Zhang, Y. Tao, and S. Zhai, "An image classification model for natural scenes based on model transfer learning," in *2024 5th International Conference on Geology, Mapping and Remote Sensing (ICGMRS)*, 2024, pp. 108-111, doi: 10.1109/ICGMRS62107.2024.10581023

[17] A. Mohan, A. G. -Patron, M. Pritchard, and H. Kerner, "Hotspotter: a generalizable pipeline for automated detection of subtle volcanic thermal features in satellite images," in *Proceedings of the AAAI Conference on Artificial Intelligence*, 2025, vol. 39, no. 28, pp. 28857–28863, doi: 10.1609/aaai.v39i28.35151.

[18] K. Huertas, N. P. -Pèrez, D. S. Benítez, M. B.-Calisto, M. Herrera, and O. Camacho, "Application of transformer models for volcano seismic signals classification," in *2025 IEEE Colombian Conference on Applications of Computational Intelligence (ColCACI)*, Aug. 2025, pp. 1–5, doi: 10.1109/ColCACI67437.2025.11230894.

[19] E. Amato, C. Corradino, F. Torrisi, and C. D. Negro, "SqueezeNet dataset transfer learning," *Zenodo*, v1. 2023, doi: 10.5281/zenodo.7944343

[20] K. He, X. Zhang, S. Ren, and J. Sun, "Deep residual learning for image recognition," *2016 IEEE Conference on Computer Vision and Pattern Recognition (CVPR)*, 2016, pp. 770-778, doi: 10.1109/CVPR.2016.90.

[21] B. Zoph, V. Vasudevan, J. Shlens, and Q. V. Le, "Learning transferable architectures for scalable image recognition," *2018 IEEE/CVF Conference on Computer Vision and Pattern Recognition*, 2018, pp. 8697-8710, doi: 10.1109/CVPR.2018.00907.

[22] G. Huang, Z. Liu, L. V. D. Maaten, and K. Q. Weinberger, "Densely connected convolutional networks," *2017 IEEE Conference on Computer Vision and Pattern Recognition (CVPR)*, 2017, pp. 2261-2269, doi: 10.1109/CVPR.2017.243.
[23] A. G. Howard *et al.*, "MobileNets: efficient convolutional neural networks for mobile vision applications," 2017, *arXiv:1704.04861*.
[24] C. Szegedy, V. Vanhoucke, S. Ioffe, J. Shlens, and Z. Wojna, "Rethinking the inception architecture for computer vision," *2016 IEEE Conference on Computer Vision and Pattern Recognition (CVPR)*, 2016, pp. 2818-2826, doi: 10.1109/CVPR.2016.308.
[25] F. Chollet, "Xception: deep learning with depthwise separable convolutions," *2017 IEEE Conference on Computer Vision and Pattern Recognition (CVPR)*, 2017, pp. 1800-1807, doi: 10.1109/CVPR.2017.195.
[26] K. Simonyan and A. Zisserman, "Very deep convolutional networks for large-scale image recognition," 2014, *arXiv:1409.1556*.

BIOGRAPHIES OF AUTHORS

Yasir Hussein Shakir is a software engineer and an expert in machine learning. He obtained his B.Sc. degree in Software Engineering from Baghdad College of Economic Sciences University in 2014 and his M.Sc. degree in Computer and Communication Engineering, specializing in Computer Programming, from the Faculty of Engineering at the Islamic University of Lebanon (IUL) in 2018. His research expertise spans data mining, medical image processing, medical electronic systems, machine learning, deep learning, and artificial intelligence. Currently, he is a Ph.D. student in the Department of Engineering at Universiti Tenaga Nasional (UNITEN) in Malaysia. He can be contacted at email: yasserhessein19855@gmail.com.

Reem Ali Mutlag is a computer and communication engineer. She received her B.Sc. degree in Computer and Communication Engineering from the University of Baghdad, Iraq, in 2013. She is currently pursuing her Master of Science (M.Sc.) in the Department of Electrical and Electronic Engineering at Universiti Tenaga Nasional (UNITEN), Malaysia. Her research interests include IoT networks, machine learning, deep learning, and medical image processing. She can be contacted at email: SE1085194@student.uniten.edu.my.

Eshaq Aziz Awadh AL Mandhari is a senior network administrator with more than ten years. He also worked as head of the Educational Technology Center in University of Technology and Applied Sciences-Nizwa (UTAS-Nizwa) for more than three years. He received his B.Sc. (Hons) in Computing in Systems and Networking from Institute of Technology Sligo (ITSligo), Ireland, in 2015, and M.Sc. in Computer Networking from University of Bedfordshire (UOB), United Kingdom, in 2018. Currently, he is a Ph.D. student in the Graduate School of Technology at Asia Pacific University of Technology and Innovation (APU) in Malaysia. His research interests are computer networking, computer security, cloud computing, software-defined networking, self-driving electric vehicles, machine learning, and internet of things. He can be contacted at email: eshaq.almandhari@utas.edu.om.

Mohamed Shabbir Abdulnabi is an IEEE senior member and received his Ph.D. in Computer Science (Computer Security) in 2018 and his Master's in Computer Science (Information Security) in 2012, both from the University of Malaya. His research focuses on computer and information security, including healthcare system security, applied cryptography, and anomaly detection using machine learning. He is a senior lecturer at Asia Pacific University (APU), where he also serves as the program leader for the Master of Science in Cybersecurity and the Master of Science in Digital Transformation. At APU, he supervises several Ph.D. and Master's candidates and teaches cybersecurity and digital forensics modules. He holds multiple cybersecurity certifications, such as CEH, CHFI, ISACA CSX Cybersecurity Fundamentals, and RCCE. He is actively involved in ISACA, serving as a faculty advisor for the ISACA-APU student branch. He has published numerous high-impact research papers in leading international journals and conferences. He can be contacted at email: mohamed.shabbir@apu.edu.my.